ANNUAL REVIEWS

Annual Review of Neuroscience

Functional Ultrasound Neuroimaging

Gabriel Montaldo,[1] Alan Urban,[1,2] and Emilie Macé[3,4]

[1]Neuro-Electronics Research Flanders, Vlaams Instituut voor Biotechnologie, and Interuniversity Microelectronics Centre, Leuven, Belgium; email: gabriel.montaldo@nerf.be

[2]Department of Neuroscience, Faculty of Medicine, Katholieke Universiteit Leuven, Leuven, Belgium

[3]Brain-Wide Circuits for Behavior Research Group, Max Planck Institute of Neurobiology, Martinsried, Germany

[4]Current address: Max Planck Institute for Biological Intelligence, In Foundation, Martinsried, Germany; email: emace@neuro.mpg.de

Annu. Rev. Neurosci. 2022. 45:491–513

The *Annual Review of Neuroscience* is online at neuro.annualreviews.org

https://doi.org/10.1146/annurev-neuro-111020-100706

Keywords

functional ultrasound, neuroimaging, neurovascular coupling, whole-brain imaging

Abstract

Functional ultrasound (fUS) is a neuroimaging method that uses ultrasound to track changes in cerebral blood volume as an indirect readout of neuronal activity at high spatiotemporal resolution. fUS is capable of imaging head-fixed or freely behaving rodents and of producing volumetric images of the entire mouse brain. It has been applied to many species, including primates and humans. Now that fUS is reaching maturity, it is being adopted by the neuroscience community. However, the nature of the fUS signal and the different implementations of fUS are not necessarily accessible to non-specialists. This review aims to introduce these ultrasound concepts to all neuroscientists. We explain the physical basis of the fUS signal and the principles of the method, present the state of the art of its hardware implementation, and give concrete examples of current applications in neuroscience. Finally, we suggest areas for improvement during the next few years.

Contents

1. INTRODUCTION 492
2. PRINCIPLES OF FUNCTIONAL ULTRASOUND IMAGING 493
   2.1. Neurovascular Coupling 493
   2.2. Detecting Blood Motion with Ultrasound 494
   2.3. Fast Ultrasound Imaging 497
   2.4. Bringing It All Together: Functional Ultrasound Imaging 498
   2.5. Resolution of Functional Ultrasound 500
   2.6. Validity of the Functional Ultrasound Signal as a Readout of Neuronal Activity 501
3. TECHNICAL EVOLUTION: FROM SINGLE-PLANE TO VOLUMETRIC FUNCTIONAL ULTRASOUND IMAGING 502
   3.1. Real-Time Imaging 502
   3.2. Tissue Motion Filtering 502
   3.3. Volumetric Functional Ultrasound Imaging 503
4. DIVERSITY OF FUNCTIONAL ULTRASOUND APPLICATIONS IN NEUROSCIENCE 504
   4.1. Head-Fixed Rodents 504
   4.2. Freely Moving Rodents 506
   4.3. Primate Research 506
   4.4. Clinical Applications 507
   4.5. Experimental Performance of Functional Ultrasound 507
5. PERSPECTIVES FOR FUNCTIONAL ULTRASOUND IMAGING 508

1. INTRODUCTION

The complexity of the brain is fueled by the fact that it performs computations across multiple scales. While the functional role of single neurons must be addressed at the microscopic level, the role of specific brain regions should be investigated at the mesoscopic level, and the role of distributed networks becomes comprehensible only at the level of the entire brain. It is at this larger scale that some of the most astonishing functions of the brain, such as learning and cognition, can be fully understood. Understanding the computations underlying large-scale circuit interactions is one of the greatest challenges for modern systems neuroscience, but breakthroughs on this front are rendered difficult by the lack of imaging tools to observe neuronal activity in the behaving full brain.

Two categories of experiments are at the forefront of this problem. First, the brains of small animals, such as the fruit fly or zebrafish, are transparent enough for the neuronal activity of their entire brain to be imaged with optical methods (e.g., Ahrens et al. 2013, Chhetri et al. 2015). Second, for bigger brains, including those of humans and other mammals, functional magnetic resonance imaging (fMRI) is the method of choice because it enables noninvasive mapping of whole-brain activity via an indirect hemodynamic signal (Logothetis 2008, Ogawa et al. 1990). However, in small mammals such as rodents, it is still technically difficult to image awake and behaving animals with fMRI. Therefore, most experiments are performed under anesthesia (Grandjean et al. 2020, Sforazzini et al. 2014).

In 2011, a new method for imaging brain activity, called functional ultrasound (fUS) imaging, was developed (Macé et al. 2011). This method uses highly sensitive ultrasound to image changes in blood volume at the capillary level as an indirect readout of neuronal activity. fUS benefits from the known advantages of ultrasound imaging: It is a safe, fast, and portable method that can image deep within the tissue. Moreover, fUS can easily be used in awake head-fixed (Macé et al. 2018) or freely moving animals (Sieu et al. 2015, Urban et al. 2015b), has a high spatiotemporal resolution (100 μm, 100 ms), and has a large field of view that can cover the entire rodent brain (Brunner et al. 2020, Rabut et al. 2019). Such characteristics are ideal for studying large-scale integration in the brain, particularly in rodents, which offer many possibilities for manipulating specific neuronal circuits. Moreover, the portability and resolution of the system are paving the way toward clinical applications (Baranger et al. 2021).

Because of these specific advantages, fUS is increasingly being adopted by the neuroscience community (Deffieux et al. 2018, Edelman & Macé 2021, Rabut et al. 2020b, Urban et al. 2017). However, the types of signal yielded by the method, and their limits, are unknown to many neuroscientists. Similarly, the hardware and software are evolving rapidly. In this review, we aim to provide a comprehensive explanation of the signal measured by fUS and of the technological implementation of the method, both of which are crucial for understanding the potential of the method and increasing its use by neuroscientists.

2. PRINCIPLES OF FUNCTIONAL ULTRASOUND IMAGING

The physiological effect exploited by fUS imaging is the neurovascular coupling that links neuronal activity and local hemodynamic changes. Our knowledge of this effect dictates the range of hemodynamic parameters that are relevant for indirect measurement of brain activity. fUS leverages this knowledge and concepts of ultrasound imaging for functional neuroimaging.

2.1. Neurovascular Coupling

It has long been known that, in the brain, an increase in neuronal activity triggers a local vasodilation, followed by a local increase in blood flow and blood volume, to fulfil the extra demand for oxygen and glucose in the activated region (Roy & Sherrington 1890). In the brain, the blood flows from arteries to smaller arterioles penetrating into the tissue, feeding a dense capillary network where the exchange of oxygen, glucose, and metabolites between blood and neurons occurs. The capillary blood is then drained out of the brain by the veins. Importantly, the deep arterioles and capillaries are at the center of the neurovascular coupling effect because they account for more than 80% of the total cerebral blood volume (Ji et al. 2021) and because they are the first vessels to dilate upon neuronal activation (Girouard 2006, Iadecola 2017, Rungta et al. 2018). These arterioles and capillaries are small vessels (with diameters ranging from 5 to 100 μm) that transport blood at velocities ranging from 0.1 to 10 mm/s in the rodent cortex (Shih et al. 2013). The dilation induces an increase in blood velocity and blood volume in these vessels, with an onset time of ∼200 ms and a peak time around 1 s after neuronal activation (Hirano et al. 2011, Silva et al. 2007). The neurovascular coupling is often characterized by a linear model, called the hemodynamic response function, that has been extensively studied in the context of fMRI (Bandettini 2014, Hillman 2014, Logothetis et al. 2001). On the basis of this knowledge, fUS imaging was designed to infer activity by imaging a hemodynamic parameter (the blood volume) inside the arterioles and capillaries at an adequate frame rate of ∼1 Hz by use of ultrasound, a type of wave that can penetrate deep into the tissues.

2.2. Detecting Blood Motion with Ultrasound

For decades, ultrasound Doppler methods have been used in clinics to measure blood velocity in large vessels of the body, such as the carotid artery or the umbilical cord (millimeters in diameter) (Szabo 2018). fUS builds on the fundamental principle of Doppler imaging.

2.2.1. The Doppler effect. The Doppler effect is usually understood as the shift in frequency (Δf) that occurs when a sound source (i.e., an ambulance siren) is moving: The sound seems to have a higher pitch when the source moves toward us and a lower pitch when it moves away from us. This effect also works for a reflected sound: When a sound is emitted by a static source and reflected by a mobile target, its frequency is shifted by $\Delta f = 2v/\mathrm{c}f_0$ when the reflector is moving toward the source and by $\Delta f = -2v/\mathrm{c}f_0$ when it is moving away from the source (here, f_0 is the frequency of the source, v is the velocity of the target in the direction of the source, and c is the speed of sound). However, to localize echoes in depth, ultrasound scanners must use short ultrasound pulses (typically two to four cycles of ultrasound at the emission frequency). It is not technically possible to directly measure Δf from these short pulses, unlike for continuous sound waves, as in the ambulance siren example. A trick used to solve this problem consists of sending multiple pulses. As the target moves, pulses are reflected with a short time delay that can be used to compute Δf indirectly. This method, called pulsed-wave Doppler (Evans & McDicken 2000), is the basis of fUS imaging. In the following subsections, we present a detailed mathematical description of this method, which is crucial for understanding how it can be used to measure hemodynamic parameters in brain microvessels.

2.2.2. Detecting a single moving red blood cell. **Figure 1*a*** illustrates how pulsed-wave Doppler works in an ideal one-dimensional case. A short ultrasound pulse is emitted in a medium containing a single moving particle (a red blood cell in our case). A short time after emitting the pulse, the ultrasound probe receives an echo from the cell. The location z of the cell is known from the echo reception time t and the speed of sound in the brain (**Figure 1*a***).

The motion of the cell can be observed when multiple pulses are emitted over time, with a period T called the pulse repetition frequency in the millisecond range. Because of the cell's motion, each echo is slightly shifted in time relative to the preceding echo, resulting in a phase shift (**Figure 1*b***). Consequently, the discrete signal obtained from a fixed depth after each pulse $s(T)$, called the Doppler signal (**Figure 1*c***), oscillates over time. As evident from the spectrum of the Doppler signal, $S(\omega)$ (**Figure 1*d***), it oscillates at a particular frequency equivalent to the classic Doppler frequency shift, $f_\mathrm{D} = \Delta f = 2v_z f_\mathrm{US}/c$, proportional to the velocity v_z of the cell in the z direction and the central frequency f_US of the ultrasound pulse. If the particle is moving away from the probe, the frequency is negative. Negative frequencies can be detected because $s(T)$ is a complex signal (obtained using a Hilbert transform of the raw ultrasound signal). In signal processing terms, using a series of pulses, what we have done is transfer (i.e., demodulate) the Doppler frequency shift from the fast ultrasound frequency (15 MHz) onto a slower frequency: the pulse repetition frequency (~kHz).

2.2.3. The complex case of the brain microvasculature. The simple case of a single moving red blood cell can be extended to more realistic configurations: a single vessel, multiple vessels, and multiple vessels embedded in a moving tissue. For a single vessel, the Doppler spectrum will resemble that of a single cell, but its intensity will be proportional to the number of cells in the vessel. Indeed, a single vessel can be modeled as a flow of cells randomly distributed in time and moving at an average velocity (**Figure 1*e***). Consequently, the spectrum of a single vessel consists in the addition of the spectrums of each cell with a random phase. The result is a spectrum with

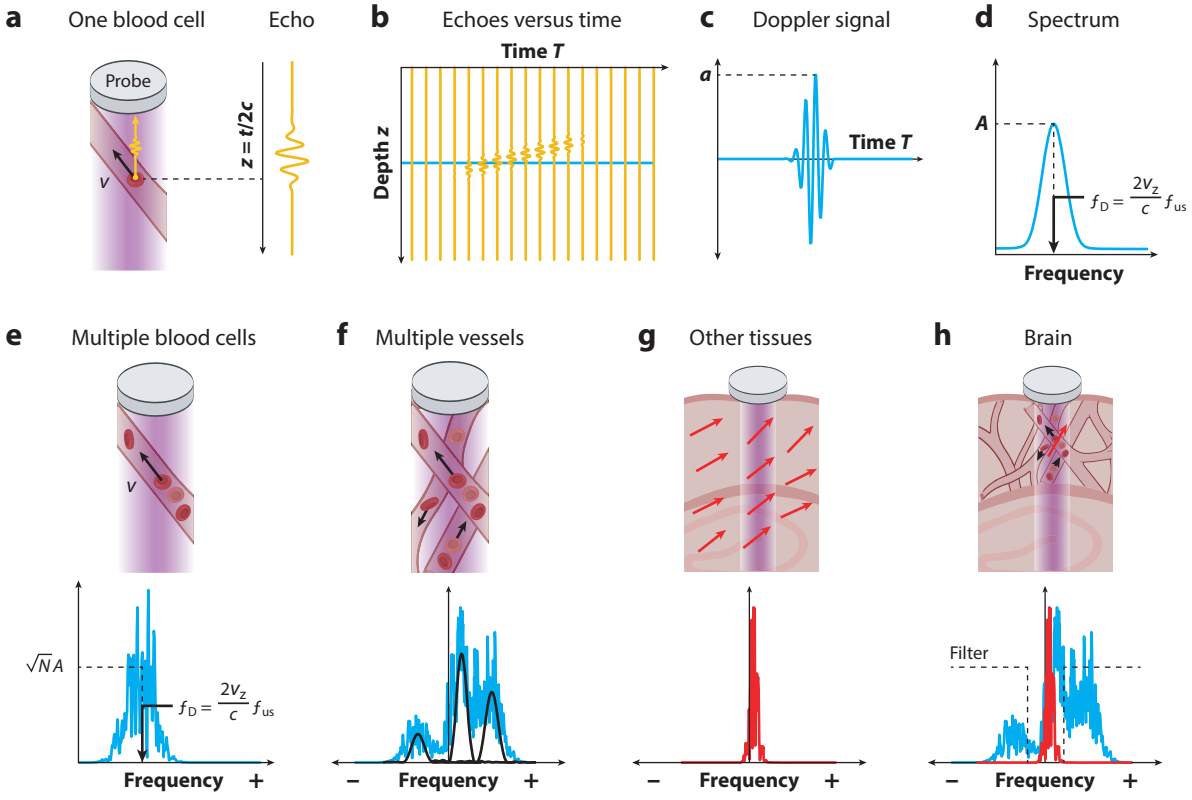

Figure 1

Detecting blood: principle of pulsed-wave Doppler in the context of brain imaging. (*a*) Case of a single moving red blood cell moving at a velocity v. A short pulse sent by an ultrasound probe hits the cell, producing an echo. The reception time of the echo gives the depth of the particle. (*b*) When a series of pulses are sent at different times T, the successive echoes are shifted in time due to the red blood cell's motion. (*c*) The signal coming from a fixed depth (represented by the *blue horizontal line* in panel *b*, e.g., from a voxel deep in the brain) is called the Doppler signal and oscillates. (*d*) The spectrum of the Doppler signal is centered around the Doppler frequency proportional to the axial velocity v_z of the cell along the z axis. (*e*) Case of a single vessel. The Doppler signals of all the cells flowing in the vessel are added, generating a spectrum with the same shape but with an amplitude $\sqrt{N}$ times higher than in the single-cell case. Spectral data were generated from a simulation. (*f*) Case of brain microvascularization. When multiple small vessels of different orientations are mixed in the same voxel, the spectra are added. Opposite flow directions generate positive and negative frequencies. However, the intensity of the spectrum is proportional to the total number of cells in the voxel or to the blood volume. Spectral data were generated from a simulation. (*g*) Other brain tissues also move but more slowly than the blood in most of the vessels, thus generating Doppler frequencies close to 0. The red arrows represent the direction and amplitude of tissue motion, which are highly correlated in neighboring voxels. Spectral data were generated from a simulation. (*h*) Realistic case of a brain voxel. The Doppler spectra from the blood and the tissue are mixed. The tissue signal must be eliminated using filtering methods. After filtering, the intensity of the spectrum is proportional to the blood volume.

the same envelope as that of a single cell but whose amplitude is multiplied by a factor $\sqrt{N}$ with respect to the single cell: $S_N(\omega) = \sqrt{N}S_1(\omega)$ (**Figure 1*e***). For this reason, the intensity of the Doppler signal, $I_N = \int S_N^2(\omega)\mathrm{d}\omega$, is proportional to the number of cells N in the voxel, $I_N = NI_1$, where $I_1 = \int S_1^2(\omega)\mathrm{d}\omega$ is the intensity of the Doppler signal from a single cell.

2.2.4. Why measure blood volume and not blood velocity? One voxel (~100 μm^3) typically includes multiple microvessels carrying blood at different velocities and in different directions. In

this case, the Doppler spectrum is the linear combination of the spectrums of the individual vessels. The Doppler spectrum becomes broad, often with positive and negative values corresponding to blood cells flowing up or down (**Figure 1*f***).

In such a situation, what is the best hemodynamic parameter to measure—blood volume or blood velocity? The intensity of the Doppler signal (linked to blood volume) continues to be proportional to *N*, the total number of moving cells in the voxel, regardless of the flow orientation. In contrast, the average Doppler frequency (linked to blood velocity) is arbitrary and unstable because there is no single peak in the spectrum. Therefore, the best way to image microvessels with heterogeneous flow directions is to measure the intensity of the Doppler signal that is proportional to the cerebral blood volume and is independent of the vessel distribution, orientation, and flow velocity (Rubin et al. 1994, 1995).

2.2.5. A source of noise: the movement of brain tissues. Blood cells are surrounded by moving brain tissues that also generate a Doppler signal. However, the movement of brain tissues (due to cardiac, breathing, and behavioral movements) is generally slow and therefore produces a Doppler signal with a lower absolute frequency than the blood (**Figure 1*g***). Use of a high-pass filter (**Figure 1*b***) enables one to eliminate the tissue signal and keep only the blood signal. The process of separating the blood and tissue signals is crucial because the tissue creates much stronger echoes (two orders of magnitude higher) than the blood. We describe more advanced filtering techniques to optimize this separation in Section 3.2. Efficient filtering is particularly important for awake recordings.

2.2.6. Physical limits of the pulsed-wave Doppler method. In summary, the pulsed Doppler method is an efficient way to quantify the number of blood cells moving inside a voxel, regardless of the type and distribution of the blood vessels. However, the principle of the method imposes specific physical constraints.

1. Depth/resolution trade-off: The spatial resolution is proportional to the pulse length (typically, two to four cycles) (**Figure 1*a***): Increasing the ultrasound frequency improves the spatial resolution. However, high frequencies have a lower penetration in tissues because of attenuation. For example, 15 MHz is a typical frequency used to image the brain of rodents (~1-cm penetration), whereas 6 MHz is used for the larger human neonate brain.
2. Pulse repetition frequency: With a 15-MHz ultrasound frequency, the Doppler frequency generated by red blood cells in brain arterioles (the fastest blood in the microvasculature) is typically 250 Hz. In order to sample this signal adequately, every voxel should be examined with a series of pulses at a minimal rate of 500 Hz.
3. Sensitivity: The echoes generated by red blood cells are very weak: They represent only 1% of amplitude of the received signal. For this reason, we need an imaging method with an excellent signal-to-noise ratio, particularly for brain voxels that usually contain both tissue and blood.

Standard ultrasound methods cannot be used in this context because they are slow and their sensitivity is too low to detect blood in the small vessels. The major technological breakthrough that enabled fUS imaging was the introduction of fast imaging methods that boosted the sensitivity to allow measurement of blood volume in very small vessels while ensuring a temporal resolution adapted to follow the hemodynamic response.

2.3. Fast Ultrasound Imaging

Pulsed-wave Doppler is the basic principle behind fUS imaging. However, its technical implementation deserves special attention, as it ultimately dictates the practical resolutions, sensitivity, and field of view of the method.

2.3.1. Hardware. The ultrasound hardware required to acquire fUS images (**Figure 2*a***) consists of three parts: a probe, a multichannel ultrasound emitter/receiver electronic device, and a computer for processing the raw data. The probe is a linear array of piezoelectric elements

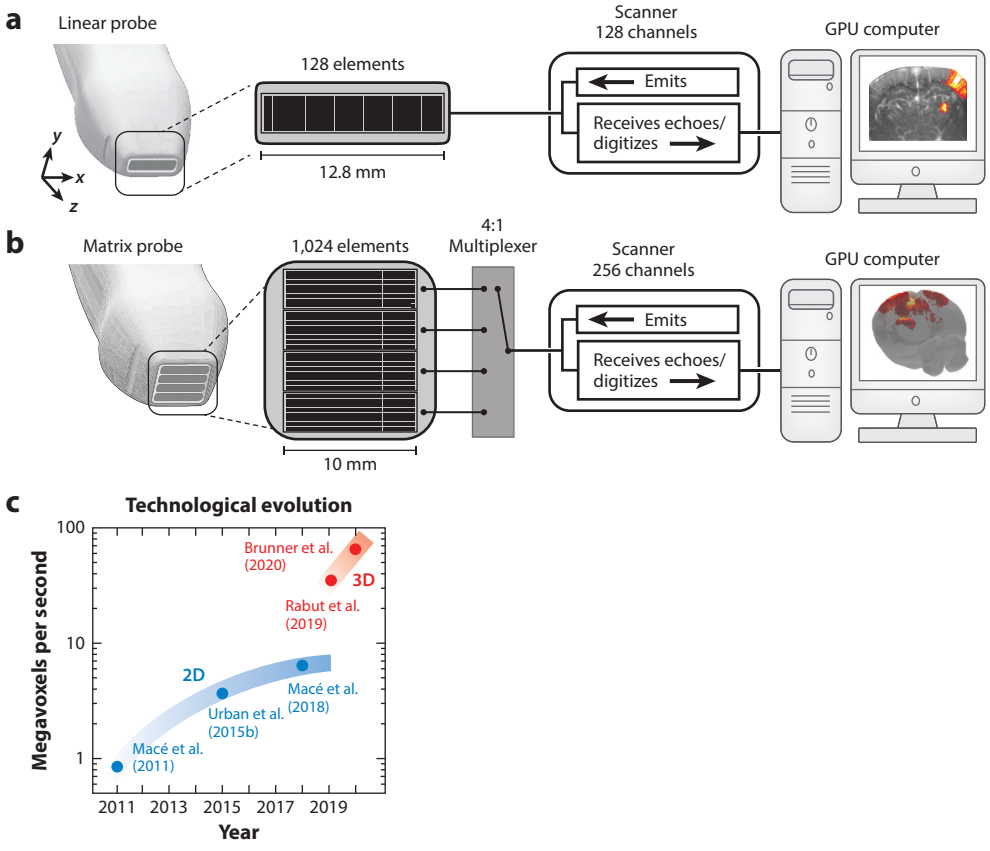

Figure 2

Hardware implementations of functional ultrasound (fUS) imaging. (*a*) Example of hardware for single-plane fUS imaging. The probe typically consists of a row of 128 piezoelectric elements spaced by 100 μm (equivalent to the wavelength for 15-MHz imaging). A 128-channel ultrasound scanner controls all probe elements, both for the emission of the ultrasound waves and for the reception of echoes. The fUS images can be reconstructed in real time inside the computer controlling the scanner, using a graphics processing unit (GPU). (*b*) Example of hardware for volumetric imaging. The probe consists of a matrix of 32 × 32 piezoelectric elements spaced by 300 μm (equivalent to three times the wavelength for 15-MHz imaging) and arranged in four sectors. The 1,024 elements of the probe are controlled by 256-channel ultrasound scanner by use of a multiplexing approach (each sector is acquired successively). The fUS images can be reconstructed in real time inside the computer controlling the scanner, using a GPU. (*c*) Technological evolution of fUS imaging, quantified as megavoxels per second acquired. While single-plane imaging has reached an optimum, volumetric imaging has boosted the recording capacity and still has room for improvement. (The papers cited represent only a subset of the literature, selected because we could compute the megavoxels-per-second value from the method details.) Panel *b* adapted with permission from Brunner et al. (2020); copyright 2018 Elsevier.

(typically 128) able to send and receive ultrasound waves. In emission mode, the electronic device can make the probe produce different ultrasound waveforms by adjusting the emission delays between the probe elements. In reception mode, the electronic device receives the echoes, digitizes the signal, and sends the data to the computer, which implements image reconstruction algorithms.

2.3.2. Standard ultrasound imaging. Standard ultrasound imaging (as performed in medical ultrasound scanners) is too slow to acquire images at the appropriate frame rate for functional brain imaging. If we imagine a typical configuration with the probe placed above a cranial window to image a coronal plane of the mouse brain (**Figure 3*a***), the standard method would use a focused ultrasound beam to image one small sector of the image and scan the medium across multiple lines and multiple depths to reconstruct the whole image (**Figure 3*b***). This scanning process takes time. For example, the time needed for an ultrasound pulse to go to a depth of 2 cm and come back to the probe is ∼30 μs ($t = 2z/c$). Therefore, to acquire one image of 128 lines and three focal depths, the theoretical limit is ∼10 ms (∼100 Hz), which is too slow for functional imaging, and requires a pulse repetition frequency of ∼500 Hz.

2.3.3. Ultrasound imaging using plane waves. Plane-wave imaging is the fastest possible way to produce an image (**Figure 3*c***). All the elements of the probe fire simultaneously, and a plane wave propagates in the whole field of view. The echoes coming from all of the particles are received and stored in memory, and an algorithm (called beamforming) can reconstruct one image on the basis of this single emission (Shattuck et al. 1984). However, because the echoes are intermixed, the images are low resolution and have a low signal-to-noise ratio.

2.3.4. Combining plane waves: the compound method. The compound method (Bercoff et al. 2011, Montaldo et al. 2009) was developed to increase the quality of the plane-wave method while keeping a high frame rate. The principle is to reconstruct a focused ultrasound beam in silico. To this end, a set of plane waves is emitted with different tilted angles (**Figure 3*d***), and each plane wave produces a low-quality image. The compound (high-quality) image results from adding these images coherently (i.e., by keeping the amplitude and phase of the images), thus recreating in every voxel the constructive and destructive interferences that would occur in the case of a focused beam. The effect of the compound method can be appreciated when comparing the point-spread functions. The plane-wave method has larger side lobes than the focused method (**Figure 3*b*,*c***), implying a loss of resolution and contrast. However, the point-spread function side lobes are tilted at different emission angles (**Figure 3*d***), resulting in destructive interference when they are added. Adding a moderate number of angles (∼10) results in a point-spread function that almost reaches the theoretical limit (Montaldo et al. 2009). Interestingly, the quality is as high as in the standard method and homogeneous across the whole image, while using fewer emissions.

Thus, the compound method fulfils all the requirements to image blood volume in small vessels: It can produce images at high frequencies (>500 Hz) with a high resolution and signal-to-noise ratio (small point-spread function). The drawback of the compound method is that it requires many computing operations. Consequently, hardware for fUS must include fast data transfer and a powerful computer unit to process the data in real time.

2.4. Bringing It All Together: Functional Ultrasound Imaging

fUS was designed to image the hemodynamic response as a proxy of neuronal activity, taking into account the constraints of the neurovascular coupling, of the pulsed-wave Doppler principle, and

of the fast imaging technology (Macé et al. 2011, 2013). The acquisition sequence consists of the following steps (**Figure 3*e***):

1. Acquiring high-quality ultrasound images at a fast rate. In the compound method, ultrasound images are acquired at a frame rate of 500 Hz, well suited for detecting blood velocities in the brain microvasculature.

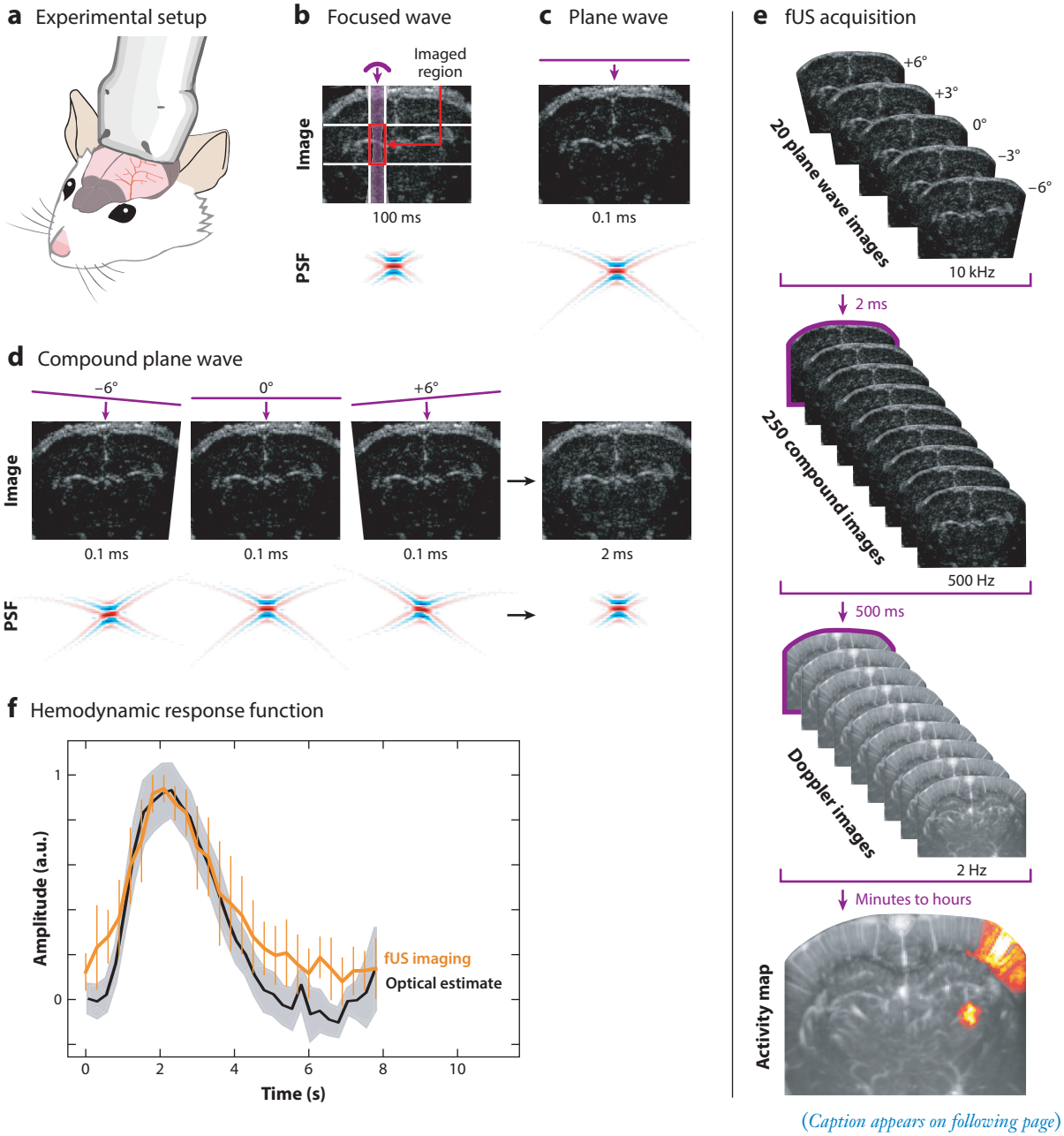

(Caption appears on following page)

Figure 3 (*Figure appears on preceding page*)

Fast ultrasound imaging and functional ultrasound (fUS) acquisition. (*a*) Schematic setup of a typical experimental configuration. The mouse is head fixed, and the ultrasound probe is placed on top of a chronic cranial window with acoustic gel to enable the ultrasound waves to penetrate into the brain. (*b*) A standard method uses focused beams of ultrasound and scans the image along multiple lines and multiple focal depths. This scan is time consuming, and the maximal imaging frequency is slow (∼100 Hz). (*c*) The use of a single plane wave and a different reconstruction algorithm enables imaging at the maximum speed (∼10 kHz). The plane-wave images are of lower quality, as illustrated by the larger point-spread function (PSF) than for the focused method. (*d*) The use of a set of tilted plane-wave emissions yields a set of different plane-wave images. The PSFs of each plane wave are different: When they are added together, the side lobes interfere destructively, and the PSF of the added image has the same quality as the optimal focused method. This compound image can be obtained at a frame rate higher than 500 Hz, adequate for Doppler imaging of cerebral microvascular blood. (*e*) Sequence of fUS imaging. There are three different timescales in an fUS sequence. First, a set of ∼10 plane-wave images is acquired at ∼10 kHz to construct a single compound image. Second, the compound image is repeated 200 times at 500 Hz to acquire the Doppler signal, and a single fUS image (or Doppler intensity image) is computed in 0.5 s. Third, the fUS image is repeated continuously to measure the changes in blood volume during brain activity. (*f*) Hemodynamic transfer function of fUS, similar to the blood volume response measured by optical methods. Panel adapted with permission from Nunez-Elizalde et al. (2022) (CC BY 4.0).

2. Measuring blood volume. Blood volume is measured in each voxel of the image from a stack of compound images using the pulsed-wave Doppler approach (filtering tissue motion and calculating the signal intensity).
3. Following changes in blood volume over time. The output of an fUS acquisition is a set of blood volume images at a frame rate of 2 to 10 Hz, depending on the desired temporal resolution of the method (see Section 2.5).

From these data, we can obtain an indirect readout of the brain activity. Importantly, akin to calcium imaging or blood-oxygen-level dependent (BOLD) fMRI, only the relative changes in fUS signal, not the amplitude itself (i.e., the average amount of blood in the voxel), are related to brain activity. Standard data analysis methods (correlation, linear models, etc.) can then be applied to these relative traces per voxel to produce, for example, a statistical activity map related to a particular stimulus (**Figure 3*e***).

2.5. Resolution of Functional Ultrasound

The spatial and temporal resolutions of fUS imaging determine the smallest hemodynamic event that can be detected.

- Temporal resolution: The size of the compound image stack (**Figure 3*e***) used to reconstruct one fUS image determines the final frame rate (50 images = 10 Hz; 250 images = 2 Hz). However, the mathematical operations made on the image stack (tissue filtering and intensity measurement) improve when using more images. Similarly to the exposure time of a camera, the user can choose the temporal resolution but makes a trade-off between speed and signal-to-noise ratio.
- Spatial resolution: The spatial resolution of fUS is intrinsically linked to the ultrasonic frequency and to the characteristics of the ultrasound probe. As an analogy, in optics the resolution is also linked to the wavelength and the characteristics of the microscope objective:
  - Single-plane imaging: For single-plane imaging, as a rule of thumb, the spatial resolution is approximately $dx = \lambda$, $dz = \lambda/2$, and dy ranges from 4λ to 10λ. The use of a 15-MHz probe yields $\lambda = 100$ μm and resolutions of ∼100, 50, and 300 μm^3 in dx, dz, and dy, respectively (Macé et al. 2018). More precisely, the resolution in depth (z axis; see **Figure 3*a***) is linked to the duration τ of the ultrasound pulse ($dz = \tau/2c$) and is constant across the whole image. The lateral resolution (x axis) is defined by the numerical aperture of the probe (i.e., the maximal angle of emission of each element):

$dx = \lambda n_{ap}$. It is constant across the whole image except near the sides, where the aperture is reduced by a factor of up to two. Finally, for single-plane imaging, the elevation resolution (or resolution off-plane; y axis) is given by the size of the ultrasound beam, which is confined to that plane by means of an acoustic lens. The resolution is calculated as $dy = \lambda F/A$, where F and A are the focal length and the size of the lens, respectively. Because the lens is designed for a fixed focal length, the image is optimal around the focal distance but degraded outside this region.

- Volumetric imaging: For volumetric imaging (see Section 3.3), the resolution is theoretically the same as for single-plane imaging: $dz = \lambda/2$ (in depth) and $dx = dy = \lambda n_{ap}$ in the two lateral dimensions (no off-plane dimension). Unfortunately, because the spacing d between the elements of the probe is greater than λ, the numerical aperture is reduced to $\sim\lambda/d$, which degrades the resolution. As a rule of thumb, with currently available matrix probes the maximum that can be achieved is on the order of $d = 300$ μm.

2.6. Validity of the Functional Ultrasound Signal as a Readout of Neuronal Activity

fUS imaging has a high spatiotemporal resolution and a large field of view, while capturing changes in blood volume in small brain vessels. However, making inferences about neuronal activity on the basis of a vascular signal is complicated.

Under the assumption of linearity, the link between neuronal activity $e(t)$ and the fUS signal $I(t)$ can be modeled as a convolution with a transfer function $h(t)$, $I(t) = e(t) * h(t)$, that can be measured experimentally. If the imaging system is perfect, then $h(t)$ is equal to the hemodynamic response function.

The transfer function of fUS has been directly measured through the use of simultaneous recordings of fUS and neuronal activity using dense multielectrode probes (Nunez-Elizalde et al. 2022). **Figure 3*f*** shows an example of this transfer function between fUS and firing rate, measured across different brain regions (visual cortex and hippocampus). This transfer function closely matches the hemodynamic response function measured in the cortex by optical imaging of total hemoglobin, an independent readout of blood volume (Pisauro et al. 2013). In parallel, the transfer function has been indirectly estimated through the (nonsimultaneous) optical measurement of calcium signals, blood velocity, and fUS signals in the olfactory bulb. This research resulted in a very similar transfer function (Aydin et al. 2020). Interestingly, the transfer function of fUS is simpler than that of the BOLD signals used in fMRI. The BOLD transfer function depends on the interplay among blood flow, blood volume, and blood oxygenation, making its modeling complex (Buxton et al. 1998). By contrast, the fUS transfer function appears monophasic and depends only on blood volume.

Collectively, these studies support the idea that the fUS signal correlates well with neuronal activity, and that this correlation can be captured by a linear filter that peaks at 2.1 s (**Figure 3*f***). Importantly, the slow transfer function implies that the relationship between fUS signals and neuronal activity becomes progressively more accurate at slower timescales (<0.5 Hz). Knowing the range of coherence between fUS signals and neuronal activity (<0.5 Hz) also guides us in choosing the appropriate filtering for the preprocessing of fUS data. Moreover, this transfer function is valid across a diverse set of brain regions (hippocampus, visual cortex, olfactory bulb), across different conditions (sensory stimulation, rest), and across animals. Although indirect, fUS signals seem to provide a robust and faithful readout of the dynamics of neuronal activity in a particular spatiotemporal range (>100 μm, <0.5 Hz).

Nonetheless, it is possible for this linear model to fail under certain conditions. First, if the hemodynamic response is impaired, for example, in a case of a pathology that could affect brain vasculature or blood pressure, the model fails (Brunner et al. 2018, Dijkhuizen et al. 2001, Girouard 2006). Second, it has been reported that strong sensory stimuli can produce a secondary, late phase of the hemodynamic response—meaning that the neurovascular coupling itself may not be linear across all stimulation regimes (Aydin et al. 2020). Finally, the transfer function of the imaging system may be degraded in the case of strong movements of the brain (because of the tissue filtering step), creating artifacts (Demené et al. 2015). Therefore, the assumptions and limitations of the transfer function should always be kept in mind when interpreting fUS results.

3. TECHNICAL EVOLUTION: FROM SINGLE-PLANE TO VOLUMETRIC FUNCTIONAL ULTRASOUND IMAGING

Initially, fUS was limited to single-plane imaging and had a low temporal resolution. Since then, fUS has undergone various technical advances to improve single-plane imaging and make volumetric imaging possible. In this section, we describe in detail these technical improvements, which have been crucial for expanding the applications of fUS in neuroscience.

3.1. Real-Time Imaging

Plane-wave imaging requires both a fast transfer of raw ultrasound data between the electronic device and the computer (up to 3 GB/s) and a high computational load. Indeed, unlike for standard ultrasound imaging, which relies on hardware image reconstruction, for fUS all the critical steps are controlled by software: storing the raw data in memory, reconstructing the compound images, filtering the tissue motion, and generating a final fUS image.

Two strategies have been implemented in practice. One strategy consists of grabbing and saving all the raw ultrasound data and applying all the processing steps after the experiment. However, this strategy limits continuous recording to only a few minutes with current saving capacities (Bergel et al. 2020, Sieu et al. 2015). Moreover, it does not allow for real-time feedback during the experiment or closed-loop paradigms.

The second strategy consists of processing the raw data in real time and saving only the compound images (at 500 Hz) or the Doppler images (at 2–10 Hz). It reduces the data flow but requires significant computing power during the experiment. In the first implementation of fUS (Macé et al. 2011), the acquisition duty cycle was only 20%, meaning that only 20% of the time was used to acquire data and the other 80% was used to compute the images. This problem has since been solved with the introduction of graphics processing units (GPUs), which dramatically accelerated the computing of the images using parallelized algorithms (Yiu et al. 2010). The use of a GPU has allowed the acquisition duty cycle to reach 100% (Brunner et al. 2020, 2021; Macé et al. 2018) (**Figure 3*f***) under real-time imaging conditions.

3.2. Tissue Motion Filtering

Improving the filtering of tissue motion represents another important advance. The blood signal generally has a higher speed (and Doppler frequency) than the surrounding tissue (**Figure 1**). However, to be efficient, the high-pass filter cutoff must be set to a minimal speed of ∼4 mm/s (75 Hz for a 15-MHz probe), which also eliminates most of the capillary signals where blood flows slowly (Shih et al. 2013). Another feature that can be used to distinguish between blood and tissue is spatiotemporal correlation. Blood echoes coming from different vessels are uncorrelated, whereas the tissue moves as a soft body, meaning that the tissue signals in neighboring voxels are

highly correlated (**Figure 1*g***). Therefore, a singular value decomposition of all brain voxels is efficient at separating the coherent movement of the tissue (identified as the principal components of the decomposition) from the incoherent blood signal (Baranger et al. 2018, Demené et al. 2015). This type of filter has also been implemented in real time inside the GPU (Brunner et al. 2020, 2021; Macé et al. 2018; Urban et al. 2015b).

3.3. Volumetric Functional Ultrasound Imaging

So far, we have focused on describing how to acquire one brain plane. However, having access to the activity of the entire brain volume is crucial in order to reveal the circuits underlying behaviors or brain functions in an unbiased way. A simple solution consists of mechanically scanning the brain plane by plane (Brunner et al. 2017, Macé et al. 2018, Sans-Dublanc et al. 2021, Sieu et al. 2015). However, the scanning time increases linearly with the number of scanned planes, and the stimulus or task must be repeated for each plane, which can lead to adaptation effects. All these problems can be solved by using a true volumetric acquisition strategy.

Volumetric imaging is conceptually no different from single-plane imaging, except that the probe consists of a 2D matrix instead of a single line of piezoelectric elements (**Figure 2*b***). The principle of compound imaging applies similarly: The matrix probe sends plane waves that propagate in the full brain volume and detects the echoes coming from the whole brain. However, the technological implementation of volumetric imaging is a major challenge. First, the matrix should ideally cover the surface of the brain (1 cm^2 in rodents) with elements separated by one wavelength for optimal resolution, which represents ∼10,000 piezoelectric elements at 15 MHz. Currently, the best probe consists of ∼1,024 elements 300 μm in size, arranged in a matrix of 32×32 that covers 1 cm^2 (**Figure 2*b***). Second, the electronic device controlling the matrix should ideally have as many channels as elements, increasing its complexity and cost. Because we can now tilt the plane waves in two directions, we must select from a larger set of angles (α_x, α_y) to perform the compound imaging and combine more plane waves to attain a similar quality of the point-spread function, which affects the acquisition speed. Finally, it is difficult to process the larger quantity of data generated in real time.

Three different implementations of three-dimensional (3D) functional imaging have been proposed. The first proof-of-concept study (Rabut et al. 2019) used the 32×32 matrix probe described above, driven by a 1,024-channel device that enables all the elements of the matrix to be addressed independently. This strategy enables full control of the ultrasound wavefront, but the frame rate (0.6 Hz), duty cycle (∼25%), and imaging duration (maximum 2.5 min) are limited by the large quantity of raw data to save. This method was tested in anesthetized rats and provided the first functional images of evoked stimulus and resting-state conditions in three dimensions.

The second study (Brunner et al. 2020) (**Figure 2*b***) used the same matrix probe, but it was driven by a 256-channel device equipped with a 4×1 multiplexer (**Figure 2*b***). This strategy relies on direct computation of the fUS images on the fly, using GPUs, which results in a higher frame rate (6 Hz), a higher duty cycle (80%), and no limitation of the imaging duration. This study followed whole-brain activity of awake head-fixed mice during visual stimulation, optogenetic stimulation, and a behavioral motor task.

In both cases, the resolution of the 3D images was lower than in the single-plane case (∼200 μm compared with 100 μm at 15 MHz; see Section 2.5). Nonetheless, the capacity to record whole-brain activity from all voxels at the same time counterbalances the loss of spatial resolution.

The third study used a different type of matrix probe (128×128 elements) in which all rows or all columns are electronically connected (Sauvage et al. 2020) and driven by a 256-channel device. This strategy reduces the number of wires, which could be interesting for specific applications

where the cable is a major issue. However, because control of the ultrasound wavefront is greatly reduced, the resulting fUS images have lower penetration, sensitivity, and spatial resolution (450 μm at 15 MHz).

Figure 2*c* summarizes the improvements of fUS technology over time, quantified as megavoxels acquired per second. The figure shows that single-plane fUS imaging reached its optimal value, that volumetric fUS imaging represents an important step for the technology, and that the plateau has not yet been reached for volumetric imaging. Therefore, there is still room for significant improvement in the next few years before fUS reaches its full power.

4. DIVERSITY OF FUNCTIONAL ULTRASOUND APPLICATIONS IN NEUROSCIENCE

Despite the method being relatively new, one clear strength of fUS is its versatility in different experimental models and conditions. In this section, we highlight concrete examples of neuroscience experiments, ranging from fundamental to clinical, that are currently feasible with fUS.

4.1. Head-Fixed Rodents

To date, most fUS studies have been performed in head-fixed rodents. Initially performed in head-fixed but anesthetized rats (Macé et al. 2011), fUS has evolved for use in head-fixed behaving mice (Macé et al. 2018) (**Figure 4*a***). These advances were enabled by protocols for long-term chronic cranial windows that are well tolerated and offer excellent imaging quality over months (Brunner et al. 2020, 2021; Kılıç et al. 2020; Macé et al. 2018). Less invasive transcranial imaging is also possible (Bertolo et al. 2021), at the cost of an important decrease in imaging quality. The shift toward awake head-fixed recordings gives rise to more motion artifacts. This problem can be minimized by improving habituation, surgical protocols, and motion filtering methods (Brunner et al. 2021).

The head-fixed configuration offers specific advantages for functional ultrasound imaging. We can image a large volume of the brain either with a 2D scanning method or with 3D volumetric imaging. Visual (Brunner et al. 2020, Gesnik et al. 2017, Macé et al. 2018), tactile (Brunner et al. 2018, 2020; Macé et al. 2011; Urban et al. 2014), and olfactive stimuli (Osmanski et al. 2014a) can easily be controlled, and the behavior can be tracked with cameras. It is also relatively easy to implant optical fibers (Brunner et al. 2020, Rungta et al. 2017, Sans-Dublanc et al. 2021) or electrodes (Macé et al. 2011, 2018; Rungta et al. 2017; Sans-Dublanc et al. 2021; Sieu et al. 2015; Urban et al. 2014) to optogenetically manipulate specific neuronal populations or to record electrical signals during the imaging session.

The first fUS studies in head-fixed anesthetized rodents aimed to demonstrate the technological capacities of fUS, usually in rats under anesthesia, for example, by mapping well-characterized sensory systems at high spatiotemporal resolution (Brunner et al. 2018, Macé et al. 2011, Rabut et al. 2019, Urban et al. 2014) or by reproducing resting-state functional connectivity experiments with fUS (Osmanski et al. 2014b **)**. A second group of studies utilized fUS in head-fixed rodents for preclinical investigation, such as for testing the effect of a drug (Ferrier et al. 2020; Rabut et al. 2020a; Vidal et al. 2020a,b), evaluating a therapeutic approach (Nayak et al. 2021, Provansal et al. 2021), or investigating different disease models (e.g., stroke, epilepsy, pain) (Brunner et al. 2017, 2018; Claron et al. 2021; Hingot et al. 2020; Macé et al. 2011; Rahal et al. 2020). Finally, recent studies in head-fixed awake mice have focused on linking behavior, circuit manipulation, and whole-brain mapping, revealing previously unknown pathways for visuomotor integration (Macé et al. 2018) or defensive behaviors (Brunner et al. 2020, Sans-Dublanc et al. 2021).

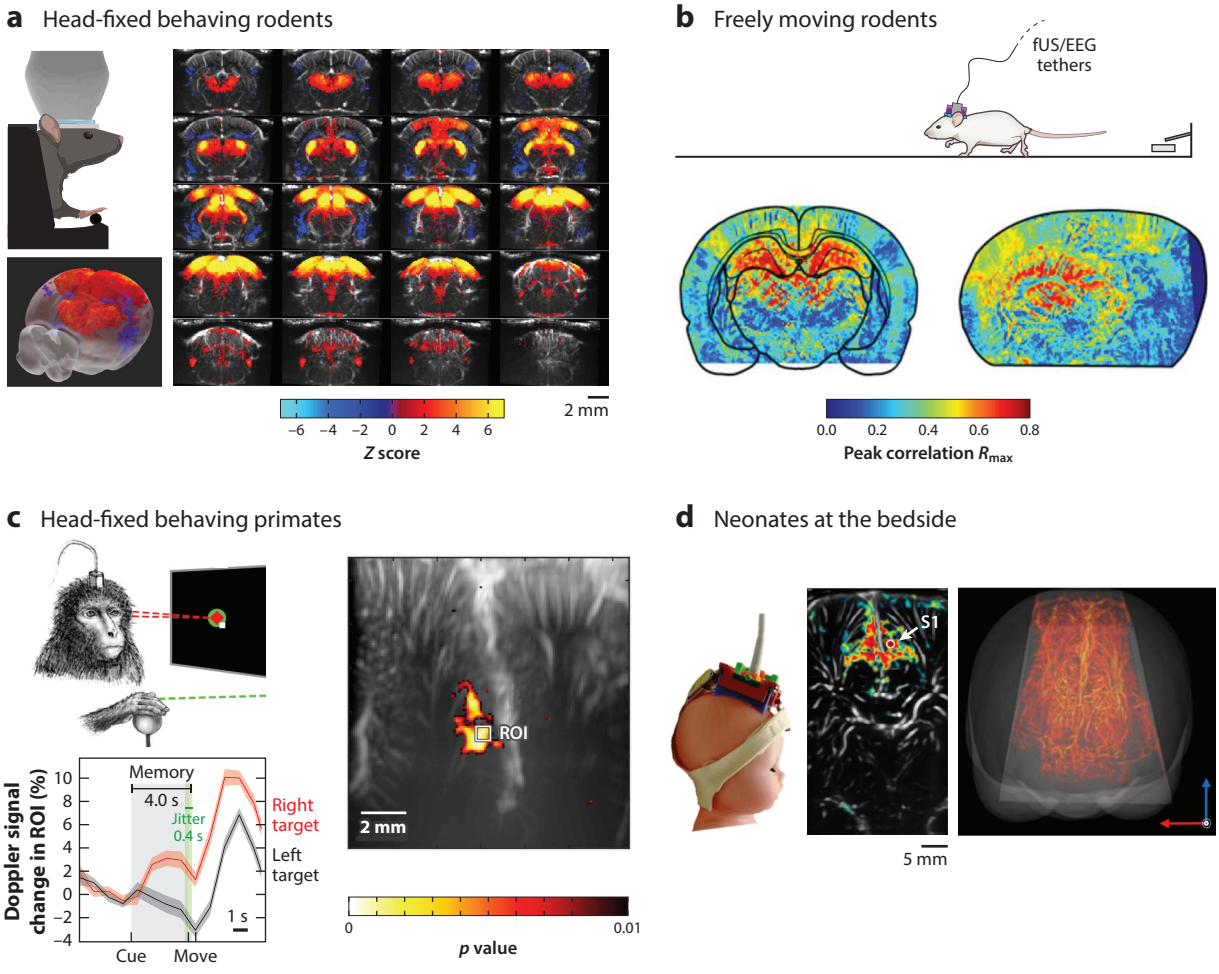

Figure 4

Examples of the applications of functional ultrasound (fUS) in neuroscience, from small animals to humans. (*a*) Imaging whole-brain activity in head-fixed behaving rodents: examples of 3D and coronal views of the regions activated during a visuomotor reflex in awake mice. (*b*) Imaging single-plane brain activity in freely moving rodents: example of the correlation maps between fUS signal and the onset of a running event in two planes of the rat brain. (*c*) Imaging activity in the deep cortex of head-fixed behaving primates: example of a decoding activity during a memory-guided motor task in macaques. The map shows a brain region significantly more active for a contralateral target (*red curve*) than an ipsilateral target (*black curve*) during the memory period before the animal moves (the time courses are from the white region of interest labeled ROI). (*d*) Imaging brain activity of neonates noninvasively at the bedside: example of a reconstructed 3D volume of the neonate vascularization imaged through the fontanelle, and the intrinsic correlation map of the fUS signal between a seed indicated by S1 and the rest of the image. Abbreviations: EEG, electroencephalography; ROI, region of interest. Panel *a* adapted with permission from Macé et al. (2011), copyright 2018 Elsevier. Panel *b* adapted from Bergel et al. (2020) (CC BY 4.0). Panel *c* adapted with permission from Norman et al. (2021), copyright 2021 Elsevier. Panel *d* adapted from Baranger et al. (2021) (CC BY 4.0).

In parallel, head-fixed imaging with fUS has been extended to other animal models of different sizes, including ferret (Bimbard et al. 2018, Landemard et al. 2021), pigeon (Rau et al. 2018), and rabbit (Demené et al. 2018), with no conceptual difference from rodents (for reviews, see Deffieux et al. 2018, Edelman & Macé 2021, Urban et al. 2017). These studies demonstrate the versatility of the method across species, as only the frequency and the probe have to be adapted for larger

brain sizes. We describe research done in primates and humans in more detail in Sections 4.3 and 4.4, below.

Notably, other parts of the nervous system can be functionally imaged in anesthetized head-fixed animals. These include the spinal cord in swine and rats (Claron et al. 2021, Song et al. 2019) and the rat trigeminal ganglion (Réaux-Le-Goazigo et al. 2022).

4.2. Freely Moving Rodents

A defining advantage of fUS is its ability to follow brain-wide activity in freely moving rodents (**Figure 4*b***). Technically, this necessitates implanting a cranial window and a holder on the head of the animal into which the ultrasound probe can be plugged for the duration of the experiment. The animal can then run or perform behavioral tasks while being connected to the ultrasound scanner through a cable.

The development of freely moving imaging relied on manufacturing linear ultrasound probes in a miniaturized case. Initially developed in rats (Bergel et al. 2018, 2020; Sieu et al. 2015; Urban et al. 2015b), the technique can also be used in mice with a smaller probe (Ferrier et al. 2020, Tiran et al. 2017). Currently, these miniaturized probes have a stiff cable and are able to image only a single imaging plane at a time. Nonetheless, they offer access to activity deep in the brain while rodents perform more naturalistic tasks than in the head-fixed context. As a comparison, while fMRI paradigms for head-fixed behaving rodents are slowly emerging (Dinh et al. 2021, Fonseca et al. 2020), freely moving conditions are out of reach.

After two initial papers demonstrating the feasibility of this technique in rats (Sieu et al. 2015, Urban et al. 2015b), freely moving fUS in rats has been used mostly for systems-level investigation of behavioral states, such as locomotion or sleep, that occur more naturally in unconstrained conditions (Bergel et al. 2018, 2020). Importantly, the latter studies coupled fUS imaging with simultaneous electrophysiology recordings, enabling correlation of large-scale hemodynamic patterns with neuronal activity in specific regions.

4.3. Primate Research

The small size of the fUS imaging setup makes it attractive for primate research (**Figure 4*c***) in comparison to fMRI, as it allows for a richer behavioral repertoire. As in rodents, fUS imaging in primates is performed through a chronic cranial chamber to access the brain, typically with a diameter of a few centimeters. To date, all primate fUS studies have used the same ultrasound probe as for rodent imaging and therefore have focused on the primate cortex, as penetration is limited at these high frequencies. Because the primate cortex is folded, fUS can help make discoveries in deep parts of the cortex that were previously optically inaccessible. Conceptually, lower frequencies could be used to image the whole brain depth (at the cost of resolution) to study subcortical structures.

So far, fUS has been used in macaques for antisaccade memory tasks (Dizeux et al. 2019) and to map ocular dominance columns of deep folds of the visual cortex (Blaize et al. 2020). Moreover, fUS holds potential for brain–machine interface applications. In a pioneering study (Norman et al. 2021) (**Figure 3*c***), an fUS signal recorded in a deep part of the cortex of macaques was used to decode the motor intention during the memory phase of a memory-guided reaching task. Although the temporal resolution is limited by the dynamics of the vascular signal (∼1 s), this first demonstration paves the way for translational applications to control robotic devices using deep-brain signals with fUS. Beyond macaques, fUS is being performed in freely moving marmosets, much smaller primates (Takahashi et al. 2021), with the same equipment as for rats. Such research is paving the way toward the study of natural behavior in primates.

4.4. Clinical Applications

The use of fUS in clinical applications merits special attention. Although ultrasound has been used to image blood flow in the body for decades, neuroimaging applications have been scarce. Now, the boost in sensitivity offered by fUS gives clinicians access to microvascular blood as well as local neuronal activity readouts. Nonetheless, because the skull is a major limitation, human applications of fUS have so far been restricted to neuroimaging during neurosurgery (Imbault et al. 2017, Soloukey et al. 2020, Urban et al. 2015a) or, in neonates, imaging through the fontanelle (Baranger et al. 2021, Demené et al. 2017, 2019) (**Figure 3*d***).

In the neurosurgery context, fUS provides a way to map the activation of important brain areas, for example, to improve the margins during tumor resection (Soloukey et al. 2020). For pediatric imaging, in neonates, fUS is completely noninvasive, as the fontanelle is transparent for ultrasound. Moreover, portability is a crucial asset, as premature babies cannot always be transported to scanner rooms. In neonates, fUS can detect epileptic seizures (Demené et al. 2017) and monitor functional brain connectivity (Baranger et al. 2021). Beyond its impact as a diagnostic tool, fUS could provide new insights into developmental processes in the human brain.

A note on safety: Even though ultrasound is a nonradiative modality, safety recommendations limit the power in order to avoid tissue heating or cavitation, a phenomenon that can create microbubbles that can damage the tissues. However, these adverse effects are not expected to occur with fUS, which operates within the safety range of standard Doppler ultrasound imaging. Indeed, fUS uses plane waves (i.e., with no focal point), so the maximal pressure in the brain tissue is lower than for standard ultrasound. Finally, fUS does not modulate brain activity; instead, it operates in a different parameter range than ultrasound neuromodulation, which requires lower frequencies (typically <500 kHz) and long pulses, resulting in higher acoustical energy (for a review, see Rabut et al. 2020b).

4.5. Experimental Performance of Functional Ultrasound

In this section, we describe a subset of studies that illustrate specific assets of fUS that are of interest for neuroscientists.

4.5.1. Spatial resolution. fUS can image specific barrels in the mouse brain (Brunner et al. 2020), ocular dominance columns in the primate (Blaize et al. 2020), and higher visual areas in the mouse brain (Macé et al. 2018).

4.5.2. Detecting single trials or events. fUS can follow the propagation of epileptic seizures (Macé et al. 2011, Rabut et al. 2019) or be used to decode motor intention during a task (Norman et al. 2021).

4.5.3. Deep imaging. fUS can reveal functional signals in deep regions, such as the amygdala (Macé et al. 2018) or a small thalamic nuclei (Sans-Dublanc et al. 2021), which were confirmed by electrophysiology in both cases.

4.5.4. Compatibility with other tools. fUS has been successfully combined with dense multielectrode arrays (Nunez-Elizalde et al. 2022, Sans-Dublanc et al. 2021) and optogenetics (Brunner et al. 2020, Edelman et al. 2021).

4.5.5. Summary. The breadth of fUS experiments performed so far confirms the utility, validity, and strengths of this method for neuroimaging in various contexts. Although fUS has not yet led

to groundbreaking discoveries about brain function, we believe that the method has reached a level where this will happen in the near future.

5. PERSPECTIVES FOR FUNCTIONAL ULTRASOUND IMAGING

The future of fUS imaging is strongly linked to new technological advances on one side and to accessibility to the neuroscience community on the other. Concerning accessibility, as fast imaging is becoming more popular in the medical field, many companies are starting to produce modular electronic devices with an expandable number of channels (from 32 to 1,024) and fast communication (>2 GB/s) at affordable prices. This diversity of hardware will be critical in helping the method to spread, as electronics currently cost approximately US$100,000. Concerning software advances, the power of the GPUs and the efficiency of the algorithms continue to increase; therefore, in a few years we can expect to reach the theoretical maximum speed for volumetric imaging.

The main remaining technological challenge for fUS imaging is to miniaturize the probes, either to build smaller headsets for freer movement and intraoperative use or to create high-density matrices for higher-resolution volumetric imaging. Unfortunately, standard probes are difficult to miniaturize because they are made from a bulk piezoelectric ceramic that is diced into smaller elements. This procedure is hard to automate, making the probes expensive, heavy, and limited in element size and wiring density.

Micromachined technologies such as capacitive micromachined ultrasound transducers (CMUTs) or piezoelectric micromachined ultrasound transducers (PMUTs) offer a promising approach. PMUTs (Jung et al. 2017) are made of deposited layers of piezoelectric material, while CMUTs (Brenner et al. 2019) are based on flexible silicon membranes. On paper, these technologies offer various advantages for fUS applications. The elements are smaller (down to a few micrometers) and can be printed in any shape on different materials, ideal for producing small and lightweight probes for implantable solutions or denser matrix probes for volumetric imaging. Such microfabrication can also include embedded electronic elements, such as multiplexers, to reduce the number of wires, or preamplifiers, to increase the signal-to-noise ratio. High-frequency linear probes based on CMUTs and PMUTs are already commercially available and are outperforming the standard technology, especially in the high-frequency band (15–25 MHz). Miniaturized probes mounted in a catheter for intravenous imaging have become a reality (Peng et al. 2021), stretchable probes have been tested in humans (Wang et al. 2021), and prototypes of matrix probes have been produced (Wygant et al. 2008). These new technologies may revolutionize the practical applications of fUS in the next few years.

Beyond technical improvements, could the mere concept of fUS evolve in the future? fUS has not fundamentally changed since its initial development: It tracks blood volume changes as a proxy of neuronal activity. New algorithms could emerge that would broaden the range of hemodynamic parameters that can be robustly recorded by fUS, such as blood velocity (Tang et al. 2021). Another promising avenue would be the use of ultrasound contrast agents to boost sensitivity (for reviews, see Heiles et al. 2021, Rabut et al. 2020b). Indeed, ultrasound contrast agents (typically microbubbles injected into the bloodstream) generate very strong echoes; even single bubbles can be easily detected. Although these microbubbles have proved very useful to create superresolved images of the microvasculature (Errico et al. 2015), their short lifetime (approximately minutes) and the need for intravenous injection have so far limited their practical interest for functional imaging. However, the recent development of air-filled protein nanostructures called gas vesicles (Shapiro et al. 2014) seems to produce a more stable Doppler signal than do microbubbles when injected in the bloodstream and could boost the sensitivity of fUS (Maresca et al. 2020), if their

lifetime can be further improved. In a paradigm shift, one could envision that such gas vesicles could be produced intracellularly in neurons and their acoustic signal modulated by the calcium concentration (Heiles et al. 2021). Such genetically encoded acoustic calcium indicators would completely reinvent the concept of fUS imaging.

DISCLOSURE STATEMENT

A.U. is the founder and a shareholder of AUTC Company, which commercializes neuroimaging solutions for preclinical and clinical research. The other authors are not aware of any memberships, affiliations, funding, or financial holdings that may be perceived as affecting the objectivity of this review.

ACKNOWLEDGMENTS

We thank Clément Brunner for editing the figures and Sara Oakeley for English corrections. The writing of this review was supported by the Max Planck Society and by grants from the Leducq Foundation (15CVD02), Research Foundation–Flanders (MEDI-RESCU2-AKUL/17/049, G091719N, and 1197818N), VIB Tech Watch (fUSI-MICE), and the internal Neuro-Electronics Research Flanders TechDev fund (3D-fUSI project).

LITERATURE CITED

Ahrens MB, Orger MB, Robson DN, Li JM, Keller PJ. 2013. Whole-brain functional imaging at cellular resolution using light-sheet microscopy. *Nat. Methods* 10(5):413–20

Aydin AK, Haselden WD, Goulam Houssen Y, Pouzat C, Rungta RL, et al. 2020. Transfer functions linking neural calcium to single voxel functional ultrasound signal. *Nat. Commun.* 11:2954

Bandettini PA. 2014. Neuronal or hemodynamic? Grappling with the functional MRI signal. *Brain Connect.* 4(7):487–98

Baranger J, Arnal B, Perren F, Baud O, Tanter M, Demené C. 2018. Adaptive spatiotemporal SVD clutter filtering for ultrafast Doppler imaging using similarity of spatial singular vectors. *IEEE Trans. Med. Imaging* 37(7):1574–86

Baranger J, Demené C, Frerot A, Faure F, Delanoë C, et al. 2021. Bedside functional monitoring of the dynamic brain connectivity in human neonates. *Nat. Commun.* 12:1080

Bercoff J, Montaldo G, Loupas T, Savery D, Mézière F, et al. 2011. Ultrafast compound Doppler imaging: providing full blood flow characterization. *IEEE Trans. Ultrason. Ferroelectr. Freq. Control* 58(1):134–47

Bergel A, Deffieux T, Demené C, Tanter M, Cohen I. 2018. Local hippocampal fast γ rhythms precede brain-wide hyperemic patterns during spontaneous rodent REM sleep. *Nat. Commun.* 9:5364

Bergel A, Tiran E, Deffieux T, Demené C, Tanter M, Cohen I. 2020. Adaptive modulation of brain hemodynamics across stereotyped running episodes. *Nat. Commun.* 11:6193

Bertolo A, Nouhoum M, Cazzanelli S, Ferrier J, Mariani J-C, et al. 2021. Whole-brain 3D activation and functional connectivity mapping in mice using transcranial functional ultrasound imaging. *J. Vis. Exp.* 168:e62267

Bimbard C, Demené C, Girard C, Radtke-Schuller S, Shamma S, et al. 2018. Multi-scale mapping along the auditory hierarchy using high-resolution functional ultrasound in the awake ferret. *eLife* 7:e35028

Blaize K, Arcizet F, Gesnik M, Ahnine H, Ferrari U, et al. 2020. Functional ultrasound imaging of deep visual cortex in awake nonhuman primates. *PNAS* 117(25):14453–63

Brenner K, Ergun AS, Firouzi K, Rasmussen MF, Stedman Q, Khuri-Yakub BP. 2019. Advances in capacitive micromachined ultrasonic transducers. *Micromachines* 10(2):152

Brunner C, Grillet M, Sans-Dublanc A, Farrow K, Lambert T, et al. 2020. A platform for brain-wide volumetric functional ultrasound imaging and analysis of circuit dynamics in awake mice. *Neuron* 108(5):861–75.e7

Brunner C, Grillet M, Urban A, Roska B, Montaldo G, Macé E. 2021. Whole-brain functional ultrasound imaging in awake head-fixed mice. *Nat. Protoc.* 16:3547–71

Brunner C, Isabel C, Martin A, Dussaux C, Savoye A, et al. 2017. Mapping the dynamics of brain perfusion using functional ultrasound in a rat model of transient middle cerebral artery occlusion. *J. Cereb. Blood Flow Metab.* 37(1):263–76

Brunner C, Korostelev M, Raja S, Montaldo G, Urban A, Baron J-C. 2018. Evidence from functional ultrasound imaging of enhanced contralesional microvascular response to somatosensory stimulation in acute middle cerebral artery occlusion/reperfusion in rats: a marker of ultra-early network reorganization? *J. Cereb. Blood Flow Metab.* 38(10):1690–700

Buxton RB, Wong EC, Frank LR. 1998. Dynamics of blood flow and oxygenation changes during brain activation: the balloon model. *Magn. Reson. Med.* 39(6):855–64

Chhetri RK, Amat F, Wan Y, Höckendorf B, Lemon WC, Keller PJ. 2015. Whole-animal functional and developmental imaging with isotropic spatial resolution. *Nat. Methods* 12(12):1171–78

Claron J, Hingot V, Rivals I, Rahal L, Couture O, et al. 2021. Large-scale functional ultrasound imaging of the spinal cord reveals in-depth spatiotemporal responses of spinal nociceptive circuits in both normal and inflammatory states. *Pain* 162(4):1047–59

Deffieux T, Demené C, Pernot M, Tanter M. 2018. Functional ultrasound neuroimaging: a review of the preclinical and clinical state of the art. *Curr. Opin. Neurobiol.* 50:128–35

Demené C, Baranger J, Bernal M, Delanoe C, Auvin S, et al. 2017. Functional ultrasound imaging of brain activity in human newborns. *Sci. Transl. Med.* 9(411):eaah6756

Demené C, Deffieux T, Pernot M, Osmanski B-F, Biran V, et al. 2015. Spatiotemporal clutter filtering of ultrafast ultrasound data highly increases Doppler and fUltrasound sensitivity. *IEEE Trans. Med. Imaging* 34(11):2271–85

Demené C, Mairesse J, Baranger J, Tanter M, Baud O. 2019. Ultrafast Doppler for neonatal brain imaging. *NeuroImage* 185:851–56

Demené C, Maresca D, Kohlhauer M, Lidouren F, Micheau P, et al. 2018. Multi-parametric functional ultrasound imaging of cerebral hemodynamics in a cardiopulmonary resuscitation model. *Sci. Rep.* 8:16436

Dijkhuizen RM, Ren J, Mandeville JB, Wu O, Ozdag FM, et al. 2001. Functional magnetic resonance imaging of reorganization in rat brain after stroke. *PNAS* 98(22):12766–71

Dinh TNA, Jung WB, Shim H-J, Kim S-G. 2021. Characteristics of fMRI responses to visual stimulation in anesthetized versus awake mice. *NeuroImage* 226:117542

Dizeux A, Gesnik M, Ahnine H, Blaize K, Arcizet F, et al. 2019. Functional ultrasound imaging of the brain reveals propagation of task-related brain activity in behaving primates. *Nat. Commun.* 10:1400

Edelman BJ, Ielacqua GD, Chan RW, Asaad M, Choy M, Lee JH. 2021. High-sensitivity detection of optogenetically-induced neural activity with functional ultrasound imaging. *NeuroImage* 242:118434

Edelman BJ, Macé E. 2021. Functional ultrasound brain imaging: bridging networks, neurons, and behavior. *Curr. Opin. Biomed. Eng.* 18:100286

Errico C, Pierre J, Pezet S, Desailly Y, Lenkei Z, et al. 2015. Ultrafast ultrasound localization microscopy for deep super-resolution vascular imaging. *Nature* 527(7579):499–502

Evans DH, McDicken WN. 2000. *Doppler Ultrasound: Physics, Instrumentation and Signal Processing*. New York: Wiley

Ferrier J, Tiran E, Deffieux T, Tanter M, Lenkei Z. 2020. Functional imaging evidence for task-induced deactivation and disconnection of a major default mode network hub in the mouse brain. *PNAS* 117(26):15270–80

Fonseca MS, Bergomi MG, Mainen ZF, Shemesh N. 2020. Functional MRI of large scale activity in behaving mice. bioRxiv 044941. **https://doi.org/10.1101/2020.04.16.044941**

Gesnik M, Blaize K, Deffieux T, Gennisson JL, Sahel JA, et al. 2017. 3D functional ultrasound imaging of the cerebral visual system in rodents. *NeuroImage* 149(1):267–74

Girouard H. 2006. Neurovascular coupling in the normal brain and in hypertension, stroke, and Alzheimer disease. *J. Appl. Physiol.* 100(1):328–35

Grandjean J, Bienert T, Hübner N, Karataş M, Mechling A, et al. 2020. Common functional networks in the mouse brain revealed by multi-centre resting-state fMRI analysis. *NeuroImage* 205(15):116278

Heiles B, Terwiel D, Maresca D. 2021. The advent of biomolecular ultrasound imaging. *Neuroscience* 474:122–33

Hillman EMC. 2014. Coupling mechanism and significance of the BOLD signal: a status report. *Annu. Rev. Neurosci.* 37:161–81

Hingot V, Brodin C, Lebrun F, Heiles B, Chagnot A, et al. 2020. Early ultrafast ultrasound imaging of cerebral perfusion correlates with ischemic stroke outcomes and responses to treatment in mice. *Theranostics* 10(17):7480–91

Hirano Y, Stefanovic B, Silva AC. 2011. Spatiotemporal evolution of the functional magnetic resonance imaging response to ultrashort stimuli. *J. Neurosci.* 31(4):1440–47

Iadecola C. 2017. The neurovascular unit coming of age: a journey through neurovascular coupling in health and disease. *Neuron* 96(1):17–42

Imbault M, Chauvet D, Gennisson J-L, Capelle L, Tanter M. 2017. Intraoperative functional ultrasound imaging of human brain activity. *Sci. Rep.* 7:7304

Ji X, Ferreira T, Friedman B, Liu R, Liechty H, et al. 2021. Brain microvasculature has a common topology with local differences in geometry that match metabolic load. *Neuron* 109(7):1168–87.e13

Jung J, Lee W, Kang W, Shin E, Ryu J, Choi H. 2017. Review of piezoelectric micromachined ultrasonic transducers and their applications. *J. Micromech. Microeng.* 27(11):113001

Kılıç K, Tang J, Erdener ŞE, Sunil S, Giblin JT, et al. 2020. Chronic imaging of mouse brain: from optical systems to functional ultrasound. *Curr. Protoc. Neurosci.* 93:e98

Landemard A, Bimbard C, Demené C, Shamma S, Norman-Haignere S, Boubenec Y. 2021. Distinct higher-order representations of natural sounds in human and ferret auditory cortex. *eLife* 10:e65566

Logothetis NK. 2008. What we can do and what we cannot do with fMRI. *Nature* 453(7197):869–78

Logothetis NK, Pauls J, Augath M, Trinath T, Oeltermann A. 2001. Neurophysiological investigation of the basis of the fMRI signal. *Nature* 412(6843):150–57

Macé E, Montaldo G, Cohen I, Baulac M, Fink M, Tanter M. 2011. Functional ultrasound imaging of the brain. *Nat. Methods* 8(8):662–64

Macé E, Montaldo G, Osmanski B-F, Cohen I, Fink M, Tanter M. 2013. Functional ultrasound imaging of the brain: theory and basic principles. *IEEE Trans. Ultrason. Ferroelectr. Freq. Control* 60(3):492–506

Macé E, Montaldo G, Trenholm S, Cowan C, Brignall A, et al. 2018. Whole-brain functional ultrasound imaging reveals brain modules for visuomotor integration. *Neuron* 100(5):1241–51.e7

Maresca D, Payen T, Lee-Gosselin A, Ling B, Malounda D, et al. 2020. Acoustic biomolecules enhance hemodynamic functional ultrasound imaging of neural activity. *NeuroImage* 209:116467

Montaldo G, Tanter M, Bercoff J, Benech N, Fink M. 2009. Coherent plane-wave compounding for very high frame rate ultrasonography and transient elastography. *IEEE Trans. Ultrason. Ferroelectr. Freq. Control* 56(3):489–506

Nayak R, Lee J, Chantigian S, Fatemi M, Chang S-Y, Alizad A. 2021. Imaging the response to deep brain stimulation in rodent using functional ultrasound. *Phys. Med. Biol.* 66:05LT01

Norman SL, Maresca D, Christopoulos VN, Griggs WS, Demené C, et al. 2021. Single-trial decoding of movement intentions using functional ultrasound neuroimaging. *Neuron* 109(9):1554–66.e4

Nunez-Elizalde AO, Krumin M, Reddy CB, Montaldo G, Urban A, et al. 2022. Neural correlates of blood flow measured by ultrasound. *Neuron*. In press

Ogawa S, Lee TM, Kay AR, Tank DW. 1990. Brain magnetic resonance imaging with contrast dependent on blood oxygenation. *PNAS* 87(24):9868–72

Osmanski B-F, Martin C, Montaldo G, Lanièce P, Pain F, et al. 2014a. Functional ultrasound imaging reveals different odor-evoked patterns of vascular activity in the main olfactory bulb and the anterior piriform cortex. *NeuroImage* 95:176–84

Osmanski B-F, Pezet S, Ricobaraza A, Lenkei Z, Tanter M. 2014b. Functional ultrasound imaging of intrinsic connectivity in the living rat brain with high spatiotemporal resolution. *Nat. Commun.* 5:5023

Peng C, Wu H, Kim S, Dai X, Jiang X. 2021. Recent advances in transducers for intravascular ultrasound (IVUS) imaging. *Sensors* 21(10):3540

Pisauro MA, Dhruv NT, Carandini M, Benucci A. 2013. Fast hemodynamic responses in the visual cortex of the awake mouse. *J. Neurosci.* 33(46):18343–51

Provansal M, Labernède G, Joffrois C, Rizkallah A, Goulet R, et al. 2021. Functional ultrasound imaging of the spreading activity following optogenetic stimulation of the rat visual cortex. *Sci. Rep.* 11:12603

Rabut C, Correia M, Finel V, Pezet S, Pernot M, et al. 2019. 4D functional ultrasound imaging of whole-brain activity in rodents. *Nat. Methods* 16(10):994–97

Rabut C, Ferrier J, Bertolo A, Osmanski B, Mousset X, et al. 2020a. Pharmaco-fUS: quantification of pharmacologically-induced dynamic changes in brain perfusion and connectivity by functional ultrasound imaging in awake mice. *NeuroImage* 222:117231

Rabut C, Yoo S, Hurt RC, Jin Z, Li H, et al. 2020b. Ultrasound technologies for imaging and modulating neural activity. *Neuron* 108(1):93–110

Rahal L, Thibaut M, Rivals I, Claron J, Lenkei Z, et al. 2020. Ultrafast ultrasound imaging pattern analysis reveals distinctive dynamic brain states and potent sub-network alterations in arthritic animals. *Sci. Rep.* 10:10485

Rau R, Kruizinga P, Mastik F, Belau M, De Jong N, Bosch J, et al. 2018. 3D functional ultrasound imaging of pigeons. *NeuroImage* 183:469–77

Réaux-Le-Goazigo A, Beliard B, Delay L, Rahal L, Claron J, et al. 2022. Ultrasound localization microscopy and functional ultrasound imaging reveal atypical features of the trigeminal ganglion vasculature. *Commun. Biol.* 5:330

Roy CS, Sherrington CS. 1890. On the regulation of the blood-supply of the brain. *J. Physiol.* 11(1/2):85–158

Rubin JM, Adler RS, Fowlkes JB, Spratt S, Pallister JE, et al. 1995. Fractional moving blood volume: estimation with power Doppler US. *Radiology* 197(1):183–90

Rubin JM, Bude RO, Carson PL, Bree RL, Adler RS. 1994. Power Doppler US: a potentially useful alternative to mean frequency-based color Doppler US. *Radiology* 190(3):853–56

Rungta RL, Chaigneau E, Osmanski B-F, Charpak S. 2018. Vascular compartmentalization of functional hyperemia from the synapse to the pia. *Neuron* 99(2):362–75.e4

Rungta RL, Osmanski B-F, Boido D, Tanter M, Charpak S. 2017. Light controls cerebral blood flow in naive animals. *Nat. Commun.* 8:14191

Sans-Dublanc A, Chrzanowska A, Reinhard K, Lemmon D, Nuttin B, et al. 2021. Optogenetic fUSI for brain-wide mapping of neural activity mediating collicular-dependent behaviors. *Neuron* 109(11):1888–905.e10

Sauvage J, Poree J, Rabut C, Ferin G, Flesch M, et al. 2020. 4D functional imaging of the rat brain using a large aperture row-column array. *IEEE Trans. Med. Imaging* 39(6):1884–93

Sforazzini F, Schwarz AJ, Galbusera A, Bifone A, Gozzi A. 2014. Distributed BOLD and CBV-weighted resting-state networks in the mouse brain. *NeuroImage* 87:403–15

Shapiro MG, Goodwill PW, Neogy A, Yin M, Foster FS, et al. 2014. Biogenic gas nanostructures as ultrasonic molecular reporters. *Nat. Nanotechnol.* 9(4):311–16

Shattuck DP, Weinshenker MD, Smith SW, von Ramm OT. 1984. Explososcan: a parallel processing technique for high speed ultrasound imaging with linear phased arrays. *J. Acoust. Soc. Am.* 75(4):1273–82

Shih AY, Blinder P, Tsai PS, Friedman B, Stanley G, et al. 2013. The smallest stroke: occlusion of one penetrating vessel leads to infarction and a cognitive deficit. *Nat. Neurosci.* 16(1):55–63

Sieu L-A, Bergel A, Tiran E, Deffieux T, Pernot M, et al. 2015. EEG and functional ultrasound imaging in mobile rats. *Nat. Methods* 12(9):831–34

Silva AC, Koretsky AP, Duyn JH. 2007. Functional MRI impulse response for BOLD and CBV contrast in rat somatosensory cortex. *Magn. Reson. Med.* 57(6):1110–18

Soloukey S, Vincent AJPE, Satoer DD, Mastik F, Smits M, et al. 2020. Functional ultrasound (fUS) during awake brain surgery: the clinical potential of intra-operative functional and vascular brain mapping. *Front. Neurosci.* 2019.01384

Song P, Cuellar CA, Tang S, Islam R, Wen H, et al. 2019. Functional ultrasound imaging of spinal cord hemodynamic responses to epidural electrical stimulation: a feasibility study. *Front. Neurol.* 10:279

Szabo TL. 2018. *Diagnostic Ultrasound Imaging: Inside Out*. Amsterdam: Elsevier

Takahashi DY, El Hady A, Zhang YS, Liao DA, Montaldo G, et al. 2021. Social-vocal brain networks in a non-human primate. bioRxiv 2021.12.01.470701. **https://doi.org/10.1101/2021.12.01.470701**

Tang J, Kılıç K, Szabo TL, Boas DA. 2021. Improved color Doppler for cerebral blood flow axial velocity imaging. *IEEE Trans. Med. Imaging* 40(2):758–64

Tiran E, Ferrier J, Deffieux T, Gennisson J-L, Pezet S, et al. 2017. Transcranial functional ultrasound imaging in freely moving awake mice and anesthetized young rats without contrast agent. *Ultrasound Med. Biol.* 43(8):1679–89

Urban A, Brunner C, Dussaux C, Chassoux F, Devaux B, Montaldo G. 2015a. Functional ultrasound imaging of cerebral capillaries in rodents and humans. *Jacobs J. Mol. Transl. Med.* 1(1):007

Urban A, Dussaux C, Martel G, Brunner C, Macé E, Montaldo G. 2015b. Real-time imaging of brain activity in freely moving rats using functional ultrasound. *Nat. Methods* 12:873–78

Urban A, Golgher L, Brunner C, Gdalyahu A, Har-Gil H, et al. 2017. Understanding the neurovascular unit at multiple scales: advantages and limitations of multi-photon and functional ultrasound imaging. *Adv. Drug Deliv. Rev.* 119:73–100

Urban A, Macé E, Brunner C, Heidmann M, Rossier J, Montaldo G. 2014. Chronic assessment of cerebral hemodynamics during rat forepaw electrical stimulation using functional ultrasound imaging. *NeuroImage* 101:138–49

Vidal B, Droguerre M, Valdebenito M, Zimmer L, Hamon M, et al. 2020a. Pharmaco-fUS for characterizing drugs for Alzheimer's disease—the case of THN201, a drug combination of donepezil plus mefloquine. *Front. Neurosci.* 14:835

Vidal B, Droguerre M, Venet L, Zimmer L, Valdebenito M, et al. 2020b. Functional ultrasound imaging to study brain dynamics: application of pharmaco-fUS to atomoxetine. *Neuropharmacology* 179:108273

Wang C, Qi B, Lin M, Zhang Z, Makihata M, et al. 2021. Continuous monitoring of deep-tissue haemodynamics with stretchable ultrasonic phased arrays. *Nat. Biomed. Eng.* 5(7):749–58

Wygant IO, Zhuang X, Yeh DT, Oralkan O, Sanli Ergun A, et al. 2008. Integration of 2D CMUT arrays with front-end electronics for volumetric ultrasound imaging. *IEEE Trans. Ultrason. Ferroelectr. Freq. Control* 55(2):327–42

Yiu BYS, Tsang IKH, Yu ACH. 2010. Real-time GPU-based software beamformer designed for advanced imaging methods research. In *2010 IEEE International Ultrasonics Symposium*, pp. 1920–23. Piscataway, NJ: IEEE